Physicochem. Probl. Miner. Process., 55(6), 2019, 1394-1400

http://www.journalssystem.com/ppmp

Physicochemical Problems of Mineral Processing

ISSN 1643-1049

Received July 25, 2019; reviewed; accepted September 1, 2019

Superhydrophobic MWCNTs/PDMS-nanocomposite materials: Preparation and characterization

Iryna Sulym [1], Adam Kubiak [2], Katarzyna Jankowska [2], Dariusz Sternik [3], Konrad Terpilowski [3], Yuriy Sementsov [1], Mykola Borysenko [1], Anna Derylo-Marczewska [3], Teofil Jesionowski [2]

[1] Chuiko Institute of Surface Chemistry of NASU, 17 General Naumov Str., 03164 Kyiv, Ukraine

[2] Poznan University of Technology, Faculty of Chemical Technology, Institute of Chemical Technology and Engineering, Berdychowo 4, PL-60965 Poznan, Poland

[3] Maria Curie-Sklodowska University, Faculty of Chemistry, M. Curie-Sklodowska Sq. 3, PL-20031 Lublin, Poland

Corresponding author: irynasulym@ukr.net (Iryna Sulym)

Abstract: The surface morphology, structure and hydrophobicity of low- and high-molecular weight poly(dimethylsiloxane) (PDMS) fluids physically adsorbed onto multi-walled carbon nanotubes (MWCNTs) at different weight percentages (5, 10, 20 and 40 wt.%), were studied employing X-ray diffraction (XRD), attenuated total reflectance Fourier transform infrared spectroscopy (ATR-FTIR), scanning electron microscopy (SEM) and measurements of contact angle with water. It was found that MWCNTs agglomerate forming voids between tubes of a broad range, while adsorption of the polymer from a hexane solution results in the expected wrapping of nanotubes with PDMS chains and, further, in filling voids, as represented by SEM data. ATR-FTIR was used to investigate the possible structural changes in the polymer nanocomposites. Based on the contact angle measurements via water drop shape analysis, MWCNTs/PDMS nanocomposites were characterized as a stable, superhydrophobic materials with the maximum contact angle (CA) equal to 152° at C_{PDMS} = 40 wt.%.

Keywords: poly(dimethylsiloxane), carbon nanotubes, polymer nanocomposites, superhydrophobicity

1. Introduction

Carbon has a phenomenal and unique ability to create an astonishing number of different compounds – over 10 million different compounds of carbon are known (Chemistry Operations, 2003). It is present in all carbonate minerals that form limestone and dolomite, as well as the pure carbon minerals, graphite, diamond, fullerene and carbon nanotubes. Since the discovery of carbon nanotubes (CNTs) in 1991 (Iijima, 1991), they have become the synonymous of nanotechnology because of their unique structural, mechanical, and electronic properties (Khalid, 2013). Moreover, in recent years, carbon nanotubes are prime candidates for application in the development of new polymer composite materials (Spitalsky et al., 2010; Sun et al., 2013; Klonos et al., 2018). One of the polymers, commonly used for designing and fabrication of hydrophobic/superhydrophobic materials is poly(dimethylsiloxane) (PDMS) (Kapridaki et al., 2013; Ramalingame et al., 2016; Zhang et al., 2017; Shetty et al., 2018). Its versatile includes thermal stability over a large temperature range, low surface tension, high flexibility, optical transparency, chemical inertness, biocompatibility, nontoxicity, a high degree of water-repellence and low cost (Maji et al., 2012). PDMS is a silicon-based organic polymer composed of a repeating $[SiO(CH_3)_2]$ units and is in rubber state at room temperature as its glass transition temperature is less than -120 ˚C (Kong et al., 2014). The carbon nanotubes (CNTs) consist of graphene sheets rolled to form a tube which exists as a single-walled (SWCNTs), a double-walled (DWCNTs) and a multi-walled (MWCNTs) carbon nanotubes depending on a number of formed layers of graphene sheets (Hembram et al., 2012). Furthermore, carbon nanotubes are able to create a

DOI: 10.5277/ppmp19057

surface in both microscale and nanoscale, owing to their rigid cylindrical nanostructure. The various techniques of incorporation of CNTs in the polymer matrices (mechanical stirring, *in-situ* polymerization, shear mixing, solvent mixing etc.) were applied for the fabrication of a new, advanced materials with multifunctional properties (Azhari et al., 2017). The interface between the MWCNTs and the poly(dimethylsiloxane) plays an important role in achieving good dispersion, such as the PDMS–CNT interfacial interactions, the so called CH-π interactions, between the methyl groups of the polymer and the π-electron rich surface of the nanotubes reported by Nishio and co-workers (Nishio et al., 1998). The purpose of the present work is to obtain nanocomposites with high hydrophobicity based on multi-walled carbon nanotubes (MWCNTs) and linear poly(dimethylsiloxane) with different molecular weights. The main attention was paid to the structural, morphological and hydrophobic properties of MWCNTs/PDMS polymer nanocomposites analyzed using XRD, ATR-FTIR, SEM techniques as well as contact angles measurements.

2. Experimental

2.1. Materials

Commercial poly(dimethylsiloxane) fluids of two molecular weights (Wacker Chemie AG, linear, $-CH_3$ terminated, code names: PDMS-100 and PDMS-12500 with $M_w \approx 3410$ and 39500 g/mol, respectively) were physically adsorbed onto multi-walled carbon nanotubes at the amount of 5, 10, 20 and 40 wt.%. MWCNTs were obtained by catalytic chemical vapour deposition (CCVD) (Kartel et al., 2016), using pyrolysis of propylene on complex metal oxide catalysts (Melezhyk et al., 2005). Before adsorption, the samples were dried at 110 °C for 2 h. A hexane solution of PDMS (1 wt.% PDMS) was prepared and different amounts of the same solution were added to fixed amounts of dry carbon material powder. The suspension was mechanically stirred and finally dried at room temperature for 48 h and then at 80 °C for 3 h. All samples with PDMS in the amount of 5, 10, 20 and 40 wt.% were in the powder form similar to pristine MWCNTs (P-MWCNTs), while pristine PDMS-100 and PDMS-12500 are liquids.

2.2. Methods

2.2.1. X-ray diffraction (XRD)

The crystalline structure of P-MWCNTs and MWCNTs/PDMS nanocomposites was determined by the X-ray diffraction (XRD) method. XRD analysis was performed at room temperature using a DRON-3M diffractometer (Burevestnik, St.-Petersburg, Russia) with Cu K_α (λ = 0.15418 nm) radiation and a Ni filter over an angular range of 10–70°. The average size of crystallites was estimated using the Scherrer equation (Jenkins et al., 1996).

2.2.2. Fourier transform infrared spectroscopy (ATR-FTIR)

Attenuated total reflectance - Fourier transform infrared (ATR-FTIR) spectra of P-MWCNTs, pristine PDMS and polymer nanocomposites were obtained using a Bruker Vertex 70 spectrometer (Germany) operating in attenuated total reflectance (ATR) mode over the wavenumber range of 4000–400 cm^{-1}, at a resolution of 4.0 cm^{-1} (number of scans: 64). This analysis was conducted using a single-reflection diamond ATR accessory (Platinum ATR, Bruker Optics GmbH).

2.2.3. Scanning electron microscopy (SEM)

The morphology of P-MWCNTs and MWCNTs/PDMS nanocomposites was analyzed using field emission Scanning Electron Microscopy employing a Quanta TM 3D FEG (FEI Company, USA) apparatus. SEM images were taken using an Everhart–Thornley Detector (ETD) operating at 30 kV in voltage.

2.2.4. Contact angle measurements

Contact angle measurements were carried out using of a Drop Shape Analysis System DSA100E (KRÜSS GmbH, Germany, accuracy ±0.01 mN/m). The calculation method (Young–Laplace) is based

on the sessile drop method, i.e. drops of water are deposited on a solid surface. The drop is produced before the measurement and has a constant volume during the measurement. After the successful fitting of the Young–Laplace equation, the contact angle was determined as the slope of the contour line at the 3-phase contact point.

2. Results and discussion

3.1. ATR-FTIR and XRD analysis of MWCNTs/PDMS nanocomposites

Figure 1 shows the ATR-FTIR spectra of pristine MWCNTs, PDMS and MWCNTs/PDMS nanocomposites. As compared to P-MWCNTs, the ATR-FTIR spectra of MWCNTs/PDMS composites show the presence of the symmetric and asymmetric stretching vibrations of C-H in the methyl groups of PDMS, which are observed at 2902 and 2956 cm^{-1}, respectively (Maji et al., 2012). The bands located at 1258 cm^{-1} and at 1410 cm^{-1} in the FTIR-ATR spectra of PDMS-100 are attributed to the symmetric and asymmetric, deformational vibrations of the $-CH_3$ groups, respectively. A wide multicomponent peak ranging from 1000 cm^{-1} to 1100 cm^{-1} corresponding to the symmetrical Si–O–Si stretching was also noted. This band is also observed for P-MWCNTs, because they contain in their composition a catalyst till to 20 wt.% (fumed silica/complex metal oxide) (Melezhyk et al., 2005). Si–C bands and rocking peaks for $Si(CH_3)_2$ are observed at 820–870 cm^{-1} and 780–815 cm^{-1} regions, respectively (Fig. 1ab). The spectra for PDMS-100 and PDMS-12500 are almost identical (Fig. 1b).

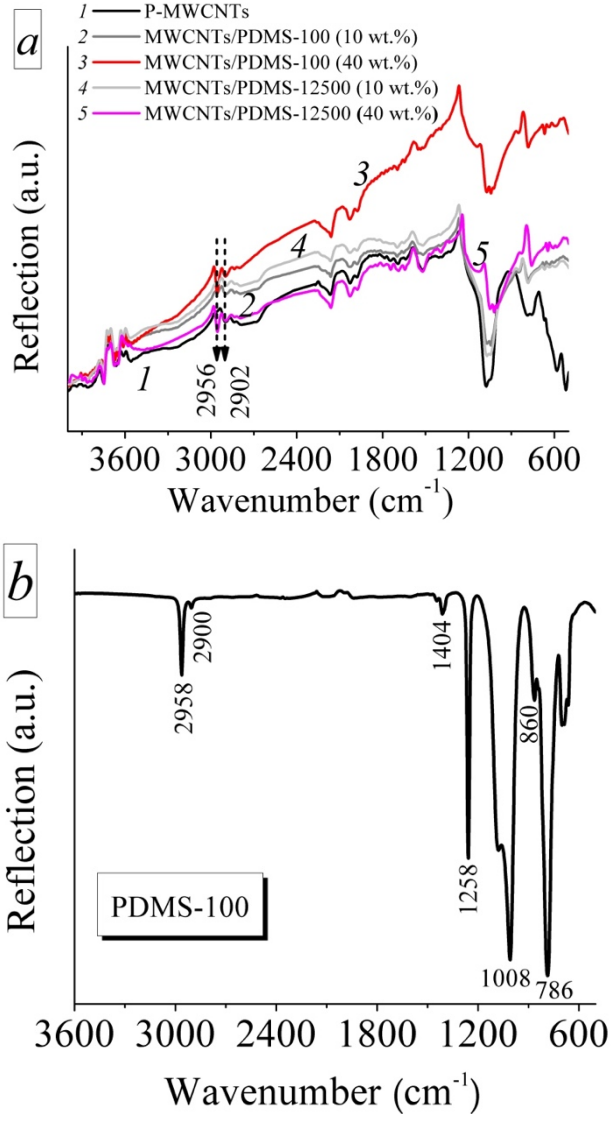

Fig. 1. ATR-FTIR spectra of P-MWCNTs and MWCNTs/PDMS nanocomposites (*a*), and PDMS-100 (*b*)

Figure 2 represents the diffraction peaks at 26.13° and 43.32°, corresponding to the graphite structure (JCPDS 41-1487) derived from MWCNTs. In addition, (002) and (100) crystal planes of carbon in MWCNTs were evaluated based on respective information from the literature (Sun et al. 2008). From the position of the peak (002), it is possible to determine the interplanar spacing (d_{002}) in the graphene layers of MWCNTs. The d_{002} value for all samples is 0.341 nm, which is more than d_{002} = 0.335 nm in well-ordered graphite. The wall thickness of MWCNTs was estimated according to the Scherrer equation from XRD (002) peak broadening. The wall thicknesses was 4 nm for all samples, and the number of graphene layers in the wall 4/0.341 (d_{002}) was approximately 12. Moreover, the position of (002) and (100) peaks of MWCNTs/PDMS composites are much closer to P-MWCNTs, this provides the evidence for the fact that the treatment does not damage the graphene layer organization. The characteristic peak of PDMS located at 12.06° (Fig. 2, *curves 2,3*) is attributed to its tetragonal phase which was confirmed according to the literature data (Kapridaki et al., 2013; Shetty et al., 2018).

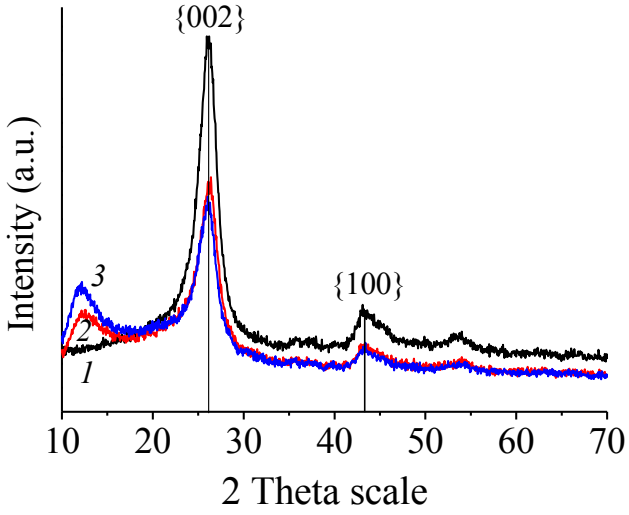

Fig. 2. XRD patterns of P-MWCNTs (*1*), MWCNTs/PDMS-100 (*2*) and MWCNTs/PDMS-12500 (*3*) nanocomposites at C_{PDMS} = 40 wt.%

3.2. Surface Morphology

The morphology of pristine MWCNTs and the fabricated MWCNTs/PDMS nanocomposites is presented in Fig. 3. These results confirm that P-MWCNTs (Fig. 3*ab*) tend to agglomerate or form bundles due to the relatively strong π-π interaction between CNT tubes (Shin at al., 2011). The images for both composites MWCNTs/PDMS-100 and MWCNTs/PDMS-12500 at C_{PDMS} = 40 wt.% show even coverage of the nanotubes surface with polymer macromolecules (Fig. 3*df*). It was observed that after modification with PDMS the average diameters of MWCNTs covered with polymer are relatively larger (45–80 nm) than that of pristine MWCNTs (10–30 nm). It was noted that an increase in concentration of PDMS from 5 to 40 wt.% leads to the formation of associates of polymer macromolecules and higher aggregation of nanotubes in nanocomposites.

3.3. Hydrophilic/hydrophobic properties of MWCNTs/PDMS nanocomposites

The hydrophobic surfaces, especially superhydrophobic surfaces (a water contact angle (CA) larger than 150°) can be used in a multitude of applications (Jeevahan et al., 2018). Evaluation of the hydrophobic properties of the composites was performed by measurements of the contact angle with water. Estimation of the apparent surface free energy (γ_S) was determined using Neumann's Equation of State (Li et al., 1992).

Using a distilled water drop of about 2 mL, CA of the samples was measured and the images for composites containing two amounts of PDMS are shown in Fig. 4. The P-MWCNTs gives CA = 57 ± 1° as a reference. It was found that CA sharply increases with adsorbed polymer content of 5 wt.%. With

further increase in PDMS content, transition range from normal hydrophobic to superhydrophobic states was proved. A stable superhydrophobic state (152 ± 1°) was reached for MWCNTs/PDMS composites with polymer concentration of 20–40 wt.%. The apparent surface free energy decreases after adsorption of both types of PDMS onto nanotubes surface and reaches a minimum (0.91 mJ/m^2) at C_{PDMS} = 40 wt.% (Fig. 4*b*). In our recent studies (Gun'ko et al., 2007; Sulym et al., 2011; Sulym et al., 2017), concerning materials prepared based on the metal oxide particles (silica, zirconia/silica, ceria–zirconia/silica) and physically adsorbed PDMS, it was shown that the composites are maximally hydrophobic (CA = 140°) at C_{PDMS} = 15–40 wt.%.

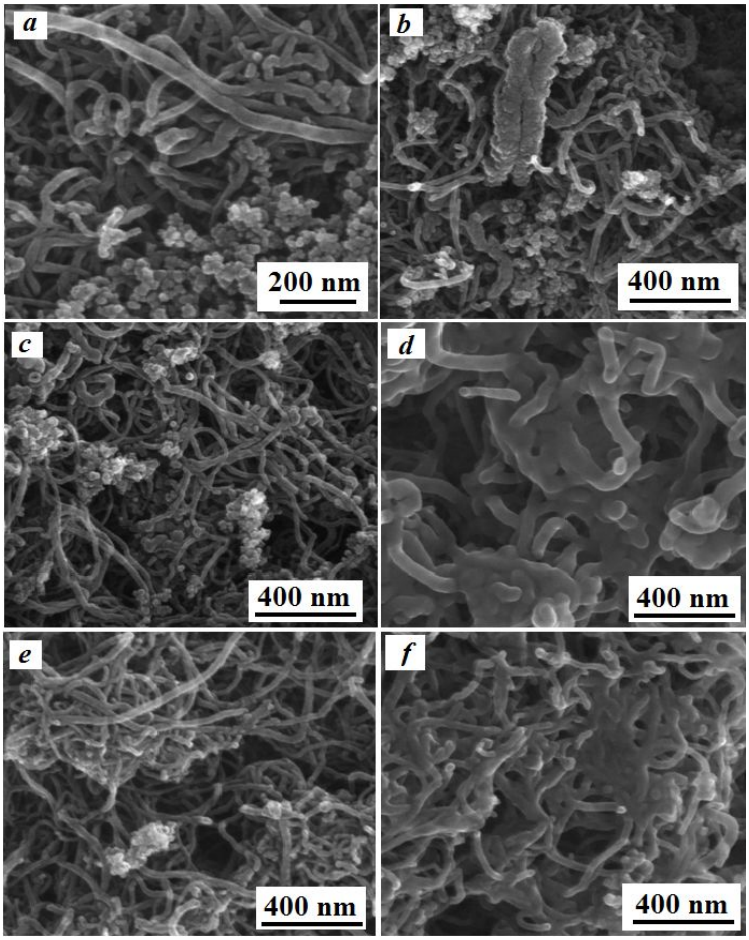

Fig. 3. SEM images of P-MWCNTs (a,b), MWCNTs/PDMS-100 at 5 wt.% (c), 40 wt.% (d) and MWCNTs/PDMS-12500 at 5 wt.% (e), 40 wt.% (f) nanocomposites

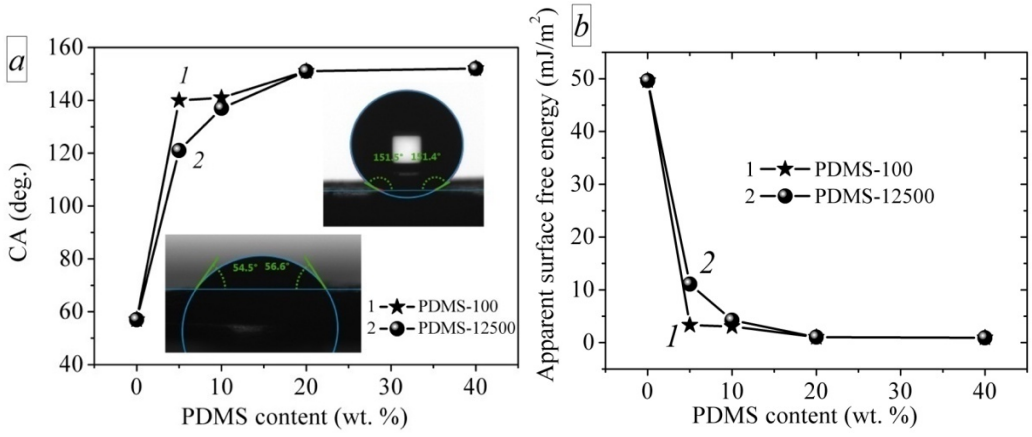

Fig. 4. Dependence of the contact angle of nanocomposites with water (a) and the apparent surface free energy (b) vs. the content of adsorbed PDMS onto MWCNTs surface

4. Conclusions

We have reported a simple method for fabricating superhydrophobic MWCNTs/PDMS nanocomposite materials. Influence of polymer content and length of PDMS chains on the surface morphology, structure and hydrophilic/hydrophobic properties of polymer nanocomposites were studied.

The analysis of ATR-FTIR spectra demonstrate the peaks at 2902 and 2956 cm^{-1} corresponding to the symmetric and asymmetric C-H stretching vibrations of the methyl groups of PDMS in MWCNTs/PDMS nanocomposites.

The SEM micrographs show that the polymer composites retain the dispersed state at the PDMS concentration of 5–40 wt.%, and well decoration of MWCNTs surfaces by PDMS molecules. The polymer is located in composites not only on the surface of MWCNTs, but also in the space between them. Moreover, it was found that the average diameter of the nanotubes increases from 10-30 nm to 45-70 nm as a result of PDMS adsorption on their surface. The smooth coverage of the MWCNTs surfaces at C_{PDMS} = 40 wt.% is more pronounced for PDMS–100, than for PDMS–12500.

The polymer nanocomposites displayed high values of the main parameters related to the hydrophobicity (CA). The contact angles of water drop for the MWCNTs/PDMS composites are about 152 degrees at C_{PDMS} = 20–40 wt.%, while for P-PDMS it is about 57 degrees. It was found that the surface free energies extremely decreased from 49.65 mJ/m^2 for P-MWCNTs to 0.91 mJ/m^2 for MWCNTs/PDMS composites with the increasing amount of PDMS. Additionally, the hydrophobicity of polymer nanocomposites is in quite close agreement with demonstrated observations by SEM method.

Acknowledgments

The authors acknowledge financial support by the Centre for East European Studies (University of Warsaw) within the framework of "NAGRODA im. I. WYHOWSKIEGO" supporting the scientific internship of Dr. I. Sulym at Poznan University of Technology and Maria Curie-Skłodowska University in Lublin as well as by the Polish Ministry of Science and Higher Education (Grant No. 03/32/SBAD/0906). The financial support of the Visegrad Fund (Contract number 51910525) is greatly appreciated.

References

AZHARI, S., YOUSEFI, A.T., TANAKA, H., KHAJEHC, A., KUREDEMUS, N., BIGDELI, M.M., HAMIDON, M.N., 2017. *Fabrication of piezoresistive based pressure sensor via purified and functionalized CNTs/PDMS nanocomposite: Toward development of haptic sensors*. Sens Actuators. A: Physical. 266, 158–165.

CHEMISTRY OPERATIONS, 2003. Carbon. Los Alamos National Laboratory. http://periodic.lanl.gov/elements/6.html/ (retrieved 2007-11-21).

GUN'KO, V.M., BORYSENKO, M.V., PISSIS, P., SPANOUDAKI, A., SHINYASHIKI, N., SULYM, I.Y., KULIK, T.V., PALYANYTSYA, B.B., 2007. *Polydimethylsiloxane at the interfaces of fumed silica and zirconia/fumed silica.* Appl. Surf. Sci. 253, 7143-7156.

HEMBRAM, K.P.S.S., MOHAN, R.G., 2012. *Origin of structural defects in multiwall carbon nanotube*. Mater Lett. 72, 68–70.

IIJIMA, S., 1991. *Helical microtubule of graphite carbon*. Nature 354, 56–58.

JEEVAHAN, J., CHANDRASEKARAN, M., JOSEPH, G.B., DURAIRA,J R.B., MAGESHWARAN, G., 2018. *Superhydrophobic surfaces: a review on fundamentals, applications, and challenges*. J. Coat. Technol. Res. 15, 231–250.

JENKINS, R., SNYDER, R.L., 1996. *Introduction to X-ray powder diffractometry*. Wiley, New York.

KAPRIDAKI, C., MARAVELAKI-KALAITZAKI, P., 2013. *TiO_2–SiO_2–PDMS nano-composite hydrophobic coating with self-cleaning properties for marble protection*. Prog. Org. Coat. 76, 400–410.

KARTEL, M., SEMENTSOV, YU., MAHNO, S., TRACHEVSKIY, V., BO, W., 2016. *Polymer composites filled with multiwall carbon nanotubes*. Univ. J. Mater. Sci. 4, 23–31.

KHALID, S.I., 2013. *Carbon nanotubes–properties and applications: a review*. Carbon Lett. 14, 131–144.

KLONOS, P., SULYM, I.Y., STERNIK, D., KONSTANTINOU, P., GONCHARUK, O.V., DERYŁO-MARCZEWSKA, A., GUN'KO, V.M., KYRITSIS, A., PISSIS, P., 2018. *Morphology, crystallization and rigid amorphous fraction in PDMS adsorbed onto carbon nanotubes and graphite*. Polymer 139, 130–144.

KONG, K.T.S., MARIATTI, M., RASHID, A.A., BUSFIELD, J.J.C., 2014. *Enhanced conductivity behavior of polydimethylsiloxane (PDMS) hybrid composites containing exfoliated graphite nanoplatelets and carbon nanotubes*. Composites Part B. 58, 457–462.

LI, D., NEUMANN, *A.W.,* 1992. *Equation of state for interfacial tensions of solid-liquid systems*. Adv. Colloid Interf. Sci. 39, 299–*345*.

MAJI, D., LAHIRI, S.K., DASA, S., 2012. *Study of hydrophilicity and stability of chemically modified PDMS surface using piranha and KOH solution*. Surf. Interf. Anal. 44, 62–69.

MELEZHYK, A.V., SEMENTSOV, YU.I., YANCHENKO, V.V., 2005. *Synthesis of thin carbon nanotubes on co-precipitated metaloxide catalysts*. Russ. J. Appl. Chem. 78, 938–946.

NISHIO, M., HIROTA, M., UMEZAWA, Y., 1998. *The CH/π interaction: evidence, nature, and consequences*. John Wiley & Sons, New York.

RAMALINGAME, R., UDHAYAKUMAR, N., TORRES, R., NECKEL, I.T., MÜLLER, C., KANOUN, O., 2016. *MWCNT-PDMS nanocomposite based flexible multifunctional sensor for health monitoring*. Procedia Eng. 168, 1775–1778.

SHETTY, H.D., PATRA, A., PRASAD, V., 2018. *Polydimethylsiloxane-multiwalled carbon nanotube composite as a metamaterial*. Mater. Lett. 210, 309–313.

SHIN, U.S., YOON, I.-K., LEE, G.-S., JANG, W.-C., KNOWLES, J.C., KIM, H.-W., 2011. *Carbon nanotubes in nanocomposites and hybrids with hydroxyapatite for bone replacements*. J. Tissue Eng. 2011, Article ID 674287, 10 pages.

SPITALSKY, Z., TASIS, D., PAPAGELIS, K., GALIOTIS, C., 2010. *Carbon nanotube–polymer composites: Chemistry, processing, mechanical and electrical properties*. Prog. Polym. Sci. 35, 357–401.

SULYM, I.Y., BORYSENKO, M.V., GONCHARUK, O.V., TERPILOWSKI, K., STERNIK, D., CHIBOWSKI, E., GUN'KO, V.M., 2011. *Structural and hydrophobic–hydrophilic properties of nanosilica/zirconia alone and with adsorbed PDMS*. Appl. Surf. Sci. 258, 270–277.

SULYM, I., GONCHARUK, O., STERNIK, D., TERPILOWSKI, K., DERYLO-MARCZEWSKA, A., BORYSENKO, M.V., GUN'KO, V.M., 2017. *Nanooxide/polymer composites with silica@PDMS and ceria–zirconia–silica@PDMS: Textural, morphological, and hydrophilic/hydrophobic features*. Nanoscale Res. Lett. 12, 152–162.

SUN, G., LI, X., QU, Y., WANG, X., YAN, H., ZHANG, Y., 2008. *Preparation and characterization of graphite nanosheets from detonation technique.* Mater. Lett. 62, 703-70.

SUN, X., SUN, H., LI, H., PENG, H., 2013. *Developing polymer composite materials: Carbon nanotubes or graphene*? Adv. Mater. 25, 5153–5176.

ZHANG, B., LI, B., JIANG, S., 2017. *Noncovalently functionalized multi-walled carbon nanotube with core-dualshell nanostructure for improved piezoresistive sensitivity of poly(dimethyl siloxane) nanocomposites*. Composites Part A. 94, 124–132.